Journal of Quantitative Spectroscopy & Radiative Transfer 273 (2021) 107838

Contents lists available at ScienceDirect

Journal of Quantitative Spectroscopy & Radiative Transfer

journal homepage: www.elsevier.com/locate/jqsrt

The spectrum of ammonia near 0.793 μm

N.F. Zobov[a], T. Bertin[b], J. Vander Auwera[b], S. Civiš[c], A. Knížek[c], M. Ferus[c], Roman I. Ovsyannikov[a], Vladimir Yu. Makhnev[a], Jonathan Tennyson[d,*], Oleg L. Polyansky[a,d,a]

[a] Institute of Applied Physics, Russian Academy of Science, Ulyanov Street 46, Nizhny Novgorod, Russia 603950
[b] Spectroscopy, Quantum Chemistry and Atmospheric Remote Sensing (SQUARES), C.P. 160/09, Université Libre de Bruxelles, 50 avenue F.D. Roosevelt, Brussels B-1050, Belgium
[c] J. Heyrovský Institute of Physical Chemistry, Czech Academy of Science, Dolejškova 2155/3, Prague 18223, Czech Republic
[d] Department of Physics and Astronomy, University College London, Gower Street, London WC1E 6BT, United Kingdom

ARTICLE INFO

Article history:
Received 11 December 2020
Revised 12 July 2021
Accepted 12 July 2021
Available online 16 July 2021

Keywords:
Ammonia
vibration-rotation spectroscopy
Fourier transform
variational calculations

ABSTRACT

Two sets of NH_3 absorption spectra covering the 0.793 μm region are recorded using two Bruker IFS 125 HR Fourier transform spectrometers. Three unapodized absorption spectra are recorded in Brussels over the range 11000 – 14500 cm^{-1} and the positions and intensities of 1114 ammonia lines observed in the 12491 – 12810 cm^{-1} region are measured using a multi-spectrum least squares fitting algorithm. 367 additional lines are identified in an ammonia absorption spectrum recorded in two steps at the J. Heyrovsky Institute of Physical Chemistry in Prague, using two different interference filters covering the 12000 – 12500 and 12400 – 13000 cm^{-1} ranges. The 1481 measured ammonia lines are analyzed using an empirical line list computed using variational nuclear motion calculations and ground state combination differences. Transitions are assigned to vibrational states with $4\nu_{NH}$ stretching excitation ($\nu_1 + \nu_3 = 4$). 278 out of the 1481 measured lines are assigned to 300 transitions and 119 upper state energy levels are derived from the frequencies of the assigned transitions.

1. Introduction

Complete characterization of ammonia molecular spectra in the microwave, infrared and optical ranges represents one of the major aims of both fundamental as well as applied high resolution molecular spectroscopy. In this field, the ammonia molecule has become a totemic system. Serendipitous observation of ammonia inversion-rotation can be found at the very beginning of this discipline [1]. The umbrella motion of ammonia is a textbook example of large amplitude motion in a molecule.

Ammonia is hazardous chemical, highly toxic for aquatic organisms, and its ever-increasing release into Earth's atmosphere has undesirable consequences [2]; monitoring its presence in the atmosphere and a detailed understanding of the nitrogen cycle is therefore a particularly important scientific objective. Remote sensing of spatially resolved atmospheric concentrations of ammonia requires reliable and extensive spectroscopic datasets and their deficiencies remain a significant source of error [3]. Ammonia is the second biggest synthetic chemical product [4,5]. NH_3 may be a biosignature gas in H_2-dominated exoplanetary atmospheres [6] or even a candidate for evidence of industrial civilization due to its relation with industry and agriculture.

Many areas in astronomy require spectroscopic data: ammonia is thought to be the key spectroscopic signature of the coldest failed stars, so-called brown dwarfs [7,8], and is probably also prominent in the atmospheres of gas giant planets both in the solar system [9] and those of other stars [10]. Indeed, Fortney et al. [11] recently suggested that hotter gas giants should show pronounced ammonia features, emphasizing the importance of characterizing highly excited vibrational states of ammonia. All these applications require accurate spectroscopic data over extended frequency and temperatures ranges. This information is also required for the analysis and assignment of hot laboratory spectra [12–16].

However, even in the relatively recent editions of HITRAN, HITRAN2008 [17], ammonia data were presented only over the limited wavenumber range below 5000 cm^{-1}. The reason for this limitation was mostly connected with the theoretical problem of accurately modelling the near IR and visible spectrum of NH_3 which

* Corresponding author.
E-mail addresses: j.tennyson@ucl.ac.uk (J. Tennyson), o.polyansky@ucl.ac.uk (O.L. Polyansky).

https://doi.org/10.1016/j.jqsrt.2021.107838

meant that spectra in these regions remained unassigned and often unanalyzed. Indeed, observations of ammonia spectra in the region around 1 μm were made at Kitt Peak in the early 1980s (C. de Bergh, unpublished). Analysis of these spectra had to wait for improvements in theory, and in particular the generation of variational line lists. These spectra have only recently been assigned [18–21]. The analogous situation arose with the spectrum of water in sunspots where detailed spectra were recorded [22] but spectral analysis [23–25] had to await variational calculations.

Returning to ammonia, recent experimental studies of the infrared spectrum include ones performed at JPL [26,27], Laboratoire de Physique Moléculaire [28], Lille-Bratislava [29], Bruxelles [30,31] as well as on Kitt Peak itself [32]. The latest edition of HITRAN, HITRAN2016 [33] includes ammonia spectra up to 10 000 cm^{-1}. The need to improve the representation of the data in ammonia is illustrated by a recent study of the visible spectrum of ammonia on Jupiter [9] which showed that the CoYuTe variational line list [34] gave a good representation of the shape of the observed features but showed a shift in wavelength which can be attributed to the lack of experimental energy levels to which the line list could be tuned. This behavior is also found in our analysis below. A review of experimental spectroscopic studies on $^{14}NH_3$ up to 7500 cm^{-1} is given as part of MARVEL (Measured Active Rotation-Vibrational Energy Levels) studies of ammonia energy levels [35,36]. At higher wavenumbers double resonance studies performed in the 1980s by Coy and Lehmann [37–39] probed ammonia levels in the 15 000 – 18 000 cm^{-1} region as did dye laser experiments by Kuga et al. [40], and the work of Giver et al. [41]. Recent work has actually managed to assign portions of these spectra up to 18 000 cm^{-1} [20]. However, there remains a conspicuous gap in the region around 12 000 cm^{-1} due, in this case, to the absence of high resolution laboratory measurements, not theory. In this paper, we report new spectra which span this gap.

This paper is organized as follows. Section 2 gives experimental details for both Brussels and Prague observations of ammonia in the 12 000 cm^{-1} spectral region. Section 3 presents the spectral analysis, the results of line assignment and the derived energy. Section 4 concludes this paper.

2. Experimental details

Fourier transform spectra of ammonia were recorded around 12 000 cm^{-1} in two different laboratories, in Brussels and in Prague. The recording and analysis of the spectra carried out in both laboratories are described below. These experiments resulted in the measurement of the positions and intensities of about 1500 ammonia lines in the 12491 – 12810 cm^{-1} spectral range.

2.1. Brussels spectra

2.1.1. Recording of the spectra

Unapodized absorption spectra of water vapor (used to calibrate the wavenumber scale) and ammonia (Fig. 1) were recorded in the range 11000 – 14500 cm^{-1} using a Bruker IFS 120HR upgraded to 125HR high resolution Fourier transform spectrometer (FTS). The instrument was fitted with a Tungsten source, a source aperture diameter of 1.7 mm, a Quartz VIS beamsplitter, a high-pass (in wavenumber) filter with a cut-off wavenumber at 11000 cm^{-1} and a Si photodiode. Both samples were contained in a White-type Pyrex multipass cell set to provide an absorption path length of 34.5 (1) meters. The cell was closed by two 2.5-mm thick CaF_2 windows and coupled under vacuum to the instrument with an appropriate transfer optics. It was operated at room temperature, defined by an air conditioning system.

The temperature of the cell was measured using four Lakeshore Pt-111 sensors fixed at different locations on the outside wall of the cell and powered by a Lakeshore model 224-12 temperature monitor. The cell and temperature sensors were wrapped in an insulating polystyrene shield. Three sensors used standard curves implemented in the temperature monitor, providing an unstated ("reasonable" according to Lakeshore) accuracy, and one of the sensors was calibrated by the manufacturer with a stated accuracy better than 0.1 K. The temperatures measured by 3 sensors, including the calibrated one, agreed within 0.1 K, while the temperature measured by the Pt-111 sensor closest to the FTS was about 0.4 – 0.6 K lower. The average temperature associated with the recording of the ammonia spectra was equal to 297(1) K, where the number between parentheses is the accuracy estimated as the sum in quadratureof half of the peak-to-peak variations measured during the recording of the interferograms and the largest difference measured between the readings of the 4 sensors (*i.e.* 0.6 K).

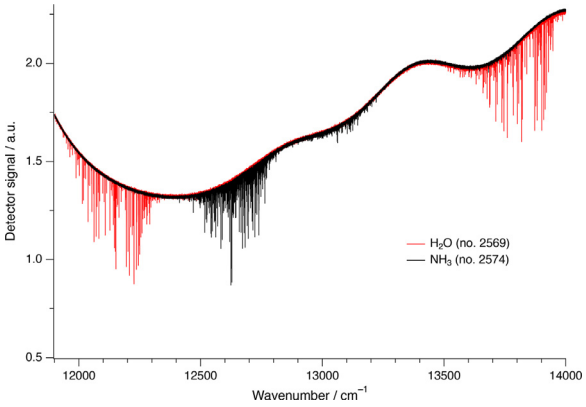

Fig. 1. Two of the spectra of water vapor and ammonia recorded in Brussels (the numbers refer to Table 1).

The water (tap water, degased by pumping for a few hours on the sample frozen with an ice/NaCl bath) vapor pressure was measured using a MKS Baratron manometer model 626 of 10 Torr full scale range. The ammonia (anhydrous, purity ≥ 99.99%, purchased from Aldrich) pressure was measured using a MKS Baratron manometer model 390HA of 100 Torr full scale range, temperature controlled at 45 °C and characterized by an accuracy of reading conservatively assumed to be 0.5%. The pressure of water vapor and ammonia evolved with time, most probably as a result of adsorption on the walls of the cell. For both samples, the recording of the spectra was started about 4 hours after filling. The uncertainties on the average pressures listed in Table 1 were estimated as the sum in quadrature of half of the peak-to-peak variations measured during the recording of the interferograms and the 0.5% accuracy of reading. The larger uncertainties reported for the NH_3 spectra numbers 2572 and 2573 are a result of the larger decrease in ammonia pressure observed for these two higher pressure samples.

All the interferograms were recorded with a scanner velocity of 20 kHz and a maximum optical path difference (MOPD) of 22.5 cm, leading to a spectral resolution of 0.04 cm^{-1}. The numbers of interferograms averaged to yield the single beam spectra are provided in Table 1. Transmittance spectra of H_2O and NH_3 were generated from the ratio of the sample spectra with empty cell spectra recorded at a resolution of 2 cm^{-1} and resulting from the co-addition of 10,000 interferograms. They were interpolated 4 times.

2.1.2. Measurements of line positions and intensities

The positions of water vapor lines observed in the ranges 11962 – 12296 cm^{-1} and 13662 – 13938 cm^{-1} in the 3 spectra recorded at the same conditions as the ammonia spectra (except

Table 1
Sample, average total pressures (P), absorption path lengths (L), temperatures (T), numbers of co-added interferograms (#), maximum optical path differences (δ_{max} in cm; the spectral resolution is equal to $0.9/\delta_{max}$) and spectral range for the spectra recorded in Prague and Brussels. The numbers between parentheses are the accuracies of measurement, provided in the units of the last quoted digit (see text for details).

Sample	No.	P / Torr	L / m	T / K	#	δ_{max}	Range / cm^{-1}
Prague							
NH_3		2	16	296	800	90.0	10000 – 16500
		2	16	296	800	90.0	12000 – 12500
		2	16	296	800	90.0	12400 – 13000
Brussels							
H_2O	2567	2.48 (31)	34.5 (1)	297 (1)	6300	22.5	11000 – 14500
	2568	8.31 (41)	34.5 (1)	297 (1)	7500	22.5	11000 – 14500
	2569	3.79 (4)	34.5 (1)	297 (1)	10,000	22.5	11000 – 14500
NH_3	2572	26.6 (1.4)	34.5 (1)	297 (1)	8650	22.5	11000 – 14500
	2573	48.2 (1.7)	34.5 (1)	297 (1)	17,400	22.5	11000 – 14500
	2574	16.77 (37)	34.5 (1)	297 (1)	20,000	22.5	11000 – 14500

for the pressures; see Table 1) were measured using the program `WSpectra` [42], giving each line a Voigt profile and including instrumental effects as fixed contributions. To determine the value of the calibration factor C (such that $\tilde{\nu}_{ref} - \tilde{\nu}_{obs} = C\ \tilde{\nu}_{obs}$) to be applied to the ammonia line positions, the measured positions $\tilde{\nu}_{obs}$ of water vapor lines were matched to the most accurate reference line positions $\tilde{\nu}_{ref}$ available in HITRAN (uncertainty code = 4, *i.e.* uncertainties in the range $10^{-4} - 10^{-3}$ cm^{-1}) [33]. The RMS deviations of the fits (involving 34, 105 and 52 line positions in spectra nos. 2567 to 2569 listed in Table 1, respectively) were in the range $4.7 - 5.2 \times 10^{-4}$ cm^{-1}. The weigthed average of the 3 values obtained for the calibration factor, *i.e.* $C = -4.7322\,(286)\ 10^{-7}$, was used to calibrate the NH_3 line positions.

The positions and intensities of ammonia lines were retrieved simultaneously from the 3 spectra, assuming that they are the same in the 3 spectra, using a multi-spectrum fitting program developed in Brussels [43,44]. This program adjusts a synthetic spectrum to each of any number of observed Fourier transform spectra, using a Levenberg-Marquardt non-linear least-squares fitting procedure. Each synthetic spectrum, interpolated 4 times with respect to the observed spectrum, is calculated as the convolution of the molecular transmission spectrum with an instrument line shape (ILS) function. The latter was estimated using the method proposed by Bernardo and Griffiths [45], relying on a few isolated water vapor lines observed in the range 12062 – 12250 cm^{-1} in spectrum no. 2567 (Table 1) interpolated 16 times. The ILS thus determined was used as is during the multi-spectrum analysis of the ammonia spectra. The profile of the molecular lines was modeled using a Voigt function [46], with Gaussian width always held fixed to the value calculated for the Doppler broadening. The self-broadening coefficients of lines stronger than 6.0×10^{-25} cm/molecule were fitted, while they were fixed to 0.4319 cm^{-1}atm^{-1} (*i.e.* the average of measurements reported in [47–49]) for weaker lines. Therefore, the positions, intensities and self broadening coefficients were fitted for lines stronger than 6.0×10^{-25} cm/molecule while only the positions and intensities were fitted for weaker lines. Pressure shift was neglected in spite of the moderate ammonia pressures used because already 3 parameters were fitted for each line relying on only 3 spectra and no signature characteristic of pressure shift could be identified in the fitting residuals. The impact of this decision on the uncertainties of the measured line positions is discussed in the next paragraph. The measurements were carried out on spectral intervals about 5 cm^{-1} wide. The background in each spectrum was modeled by a polynomial expansion up to the second order.

The observed and best-fit calculated spectra of a small range in the central part of the spectrum, and the corresponding residuals are presented in Fig. 2. The residuals show that the lines are fitted to the noise level and that the peak-to-peak signal to noise ratio is around 100 for the lower pressure spectrum (no. 2574 in Table 1) and somewhat worse for the other two. Altogether, the positions and intensities of a total of 1114 NH_3 lines were measured between 12,491 and 12,810 cm^{-1}. They are provided as supplementary material. The accuracy of the measured line positions was estimated to be in the range 2 - 5.5 $\times$ 10^{-3} cm^{-1} (Fig. 3), from the sum in quadrature of their precision of measurement, the largest RMS deviation of the fit of the H_2O reference lines (5.2×10^{-4} cm^{-1}), the uncertainty of these reference lines (assumed to be equal to 10^{-3} cm^{-1}) and the contribution of pressure shift. Similarly to Sung *et al.* [50], pressure shift was crudely estimated to be approximately 1/16th of self broadening. This value, which differs from the ratio of 1/10 of Sung *et al.* [50], is the average of the ratios of self broadening to self shift coefficients calculated from the measurements reported by Aroui *et al.* [49] and Maaroufi *et al.* [51]. As pressure shift coefficients tend to vary "randomly" between positive and negative extremes (see for example Fig. 11 of Maaroufi *et al.* [51]), the contribution δd of pressure shift to the uncertainty of the reported line positions was crudely estimated as $\delta d = 0.68$ cm^{-1}atm^{-1} $\times$ $(P_{ave}/16)$ atm $\approx 1.7 \times 10^{-3}$ cm^{-1} where 0.68 cm^{-1}atm^{-1} is the upper limit of the self broadening coefficients listed in HITRAN (96% of the self broadening coefficient measured in the present work are indeed smaller than this value) and $P_{ave} = 0.0402$ atm is the average of the NH_3 pressures corresponding to the three spectra recorded in Brussels (see Table 1). The accuracy of the line intensities (Fig. 3) was estimated including their precision of measurement, the contributions of the uncertainties on the pressures, on the temperatures (through the particle density only; the contribution of the Boltzmann factor could not be evaluated because the assignments of the lines, and therefore the energy of the corresponding lower levels, were essentially unknown), on the absorption path length and on the partition function, as well as the contribution δI of the uncertainties δb on the self broadening coefficients, the latter including the precision of measurement of the self broadening coefficients and the contribution of the uncertainty on the temperature. The contribution δI in the accuracy of the line intensities of the uncertainties δb on the self broadening coefficients was estimated to be equal to $\delta I = \delta b \times 10/15$ as follows. The positions and intensities of a set of NH_3 lines were measured twice, firstly with the self broadening coefficients of these lines fixed to $b_1 = 0.4319$ cm^{-1}atm^{-1} (the origin of this value is given in the previous paragraph) leading to measured intensities I_1 and secondly with the self broadening coefficients of these lines fitted leading to measured intensities I_2 and measured self broadening coefficients b_2. The relative differences of the intensity $\delta I = 100 \times (I_2 - I_1)/I_1$ and self broadening coefficient $\delta b = 100 \times (b_2 - b_1)/b_1$ of each line were calculated, leading to a pair of values $(\delta b, \delta I)$ for each line. A plot of all pairs $(\delta b, \delta I)$ put forward a linear correlation between δb and δI,

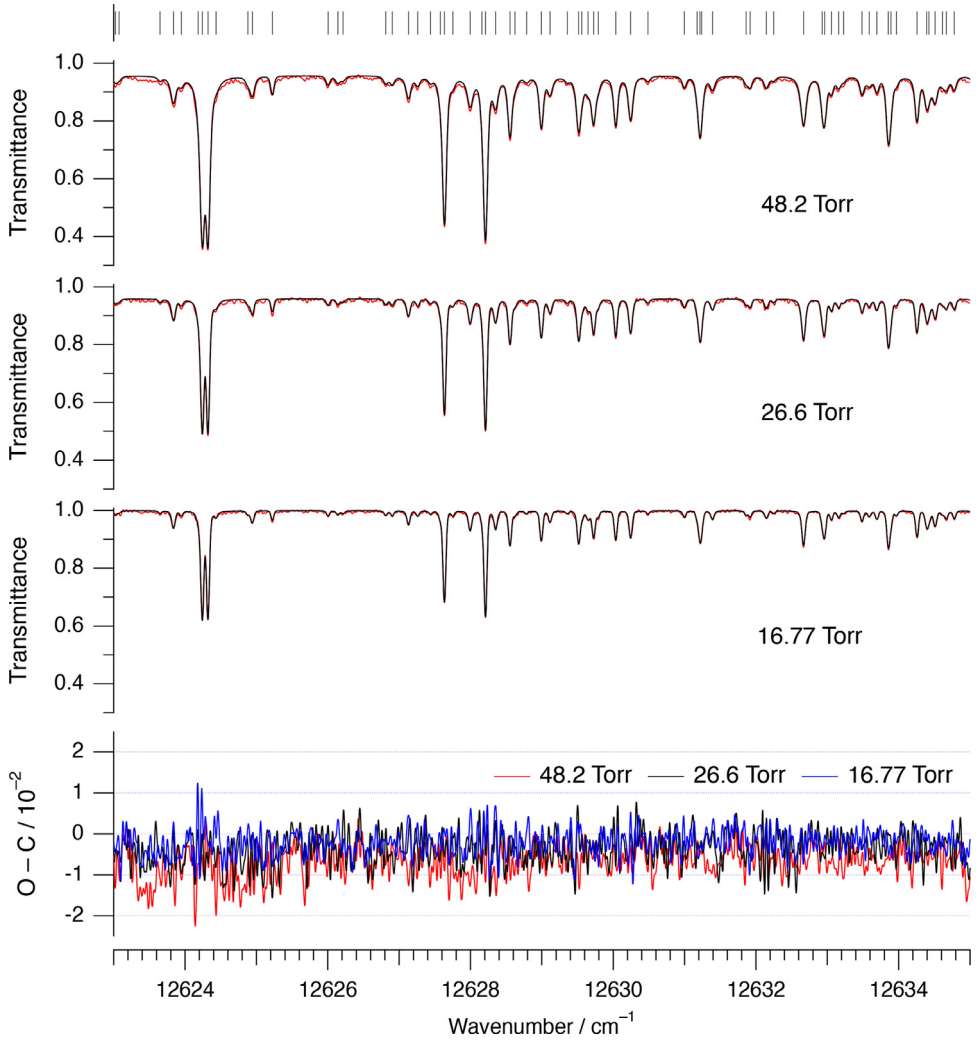

Fig. 2. Example of the measurement of the positions and intensities of NH_3 lines carried out in Brussels: Observed (red trace) and best-fit calculated (black trace) spectra of a small range in the central part of the ammonia spectrum (top 3 panels) and corresponding residuals (lower panel). The vertical bars at the top indicate the positions of fitted lines. (For interpretation of the references to colour in this figure legend, the reader is referred to the web version of this article.)

the slope of which being approximately equal to 10/15. No uncertainty information is provided for the line intensities smaller than 6.0×10^{-25} $cm^{-1}/(cm^{-2}molecule)$ as these lines are very weak in the recorded spectra and their measured intensities should be considered as estimates only. As it is not always obvious to discriminate actual lines from the noise, some of these very weak lines may actually be noise.

2.2. Prague spectra

One spectrum of ammonia was recorded at a resolution of 0.01 cm^{-1} (MOPD = 90 cm) using the Bruker IFS 125 HR Fourier transform spectrometer available at the J. Heyrovský Institute of Physical Chemistry in Prague, Czech Republic. It results from the co-addition of 800 interferograms. The instrument was equiped with a Tungsten source, a CaF_2 beam splitter, an interference filter (Spectrogon) covering the 12400 – 13000 cm^{-1} range and a Si photodiode. The ammonia sample was contained in an optical White cell, equipped with CaF_2 windows and providing an absorption path length of 16 m. The cell was connected to a side ampoule filled with ammonia and equipped with a second vacuum valve (ACE glass, USA) for gas handling and connection to the vacuum line. The pressure in the cell was 2 Torr, measured with a MKS Baratron pressure gauge (0 – 10 Torr range). The resulting spectrum is presented in Fig. 4.

The positions and relative intensities of ammonia lines observed in the recorded spectrum were measured using the OPUS software (Bruker Corporation), relying on zero crossings of the first derivative of the spectrum. The line positions thus measured were calibrated by matching the positions of 168 lines with intensities larger than 2.0×10^{-24} $cm^{-1}/(cm^{-2}molecule)$ with their calibrated positions obtained in Brussels. The line intensities were estimated by scaling the measured relative intensities with a factor determined by comparing the relative intensities measured in Prague with the integrated absorption cross section measured in Brussels for the same ammonia lines. In addition to the ammonia lines also measured in the Brussels spectra, 367 additional lines could only be observed in the Prague spectrum. Their positions and intensities are also provided as supplementary material.

3. Analysis of the spectrum

A file containing the observed line positions and intensities from the two sources is given in the supplementary data.

Spectal analysis was based on two major components: use of an accurate line list [52] and use of combination differences. The

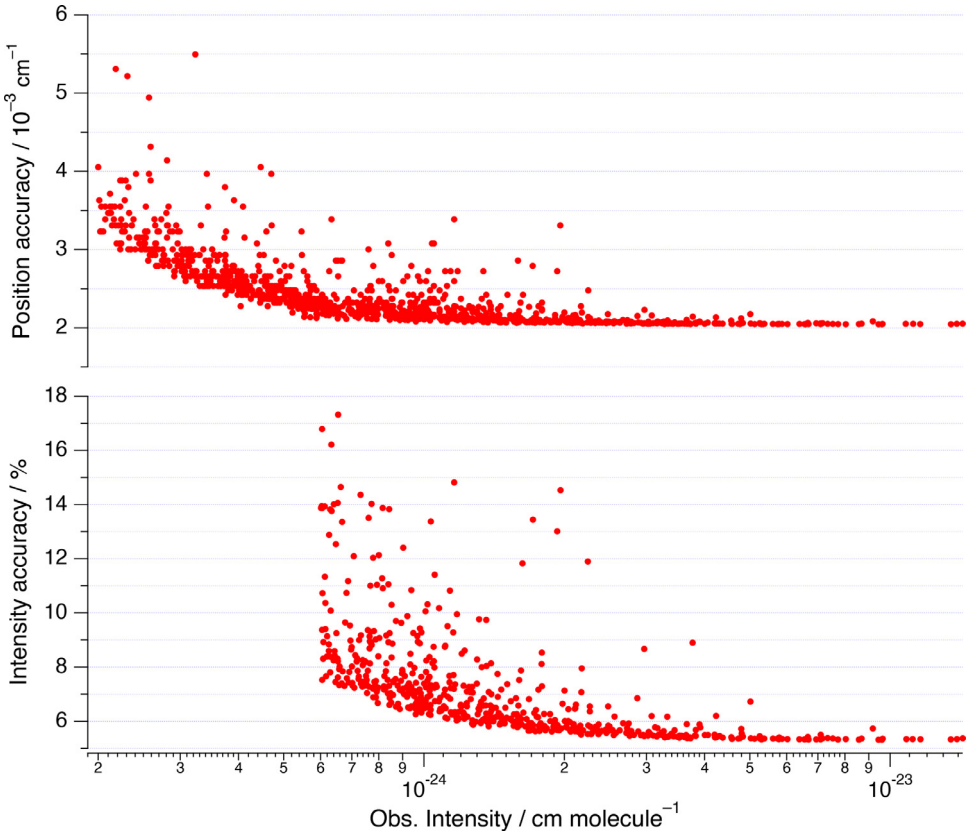

Fig. 3. Estimated accuracy of the line positions and intensities measured in the Brussels spectra. No accuracy is provided for the line intensities smaller than 6×10^{-25} $cm^{-1}/(cm^{-2}molecule)$ as the corresponding lines are very weak in the recorded spectra.

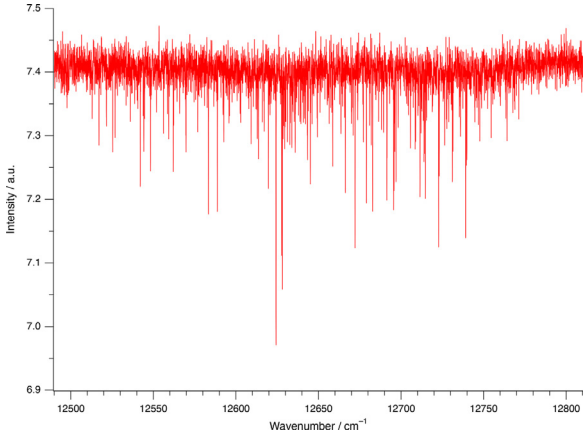

Fig. 4. Ammonia spectrum recorded in Prague, constructed from two independent measurements (800 scans, 0.01 cm^{-1} resolution) involving two different, overlapping interference filters covering the 12000 – 12500 and 12400 – 13000 cm^{-1} ranges.

Table 2
Overview of the spectral analysis carried out on the Brussels and Prague spectra.

Measured lines	1497
Assigned lines	278
Region	12491 – 12810 cm^{-1}
New experimental levels	119
New experimental levels without CD	10
Vibrational states	16
Average CD precision	0.007 cm^{-1}

success of our assignment analysis strongly depends on the accuracy of the theoretical calculations of the spectra. This accuracy is determined by the quality of the PES used for the calculations of the line list. The procedure used to adjust the PES so it reproduces the empirical energy levels is described in Ref[52]. We note that the high accuracy of the fitted PES is determined, in particular, by the high accuracy of the *ab initio* PES [53] used as a basis of this fit. The interpolation power of this PES could be demonstrated by the comparison with the subsequently observed line positions of NH_3 in the region below 10 000 cm^{-1}. The extrapolation power of this PES is demonstrated by the column "obs–calc" of Table 3. The accuracy of extrapolation is around a few wavenumbers. It proved sufficient for the assignment of the spectrum, described here below. The CD analysis based on energy values only was moderated using information on the lines intensities. We decided that combination differences were only deemed correct if the observed lines intensities differ from the theoretical ones by less than a factor of two. The intensity criterion adopted is relatively loose due to the modest accuracy of the intensities predicted in this region by the variational line list.

Analysis of the data in the 12500–12800 cm^{-1} region used a refined line list, calculated with the TROVE nuclear motion program [54] for rotational quantum numbers $J = 0 - 7$. The stronger lines in the region belong to transitions to the levels with vibrational 'TROVE quantum numbers' (0 0 4 0 0 0) and (0 0 4 0 0 1). These numbers mean that $v_1 + v_3$=4 (v_{NH}=4) and v_2=0 or 1 in standard spectroscopic ammonia vibrational quantum numbers. Calculated levels initially assigned using TROVE vibrational quantum numbers [55] were later relabeled with standard vibrational quantum numbers (v_1 v_2 v_3 L_3 v_4 L_4 L) [56]. Experimental energy levels in (0000 00 0) and (0100 00 0) vibrational states had been taken from the work of Urban et al. [57].

Table 3
Ammonia rovibrational levels derived from the line positions assigned in the $4\nu_{NH}$ region: Observed and calculated (from the refined PES) energies and corresponding differences (obs–calc), and errors in the combination differences (CD). The values listed in the 4 last columns are in cm^{-1}.

			(ν_1 ν_2 ν_3 L_3 ν_4 L_4 L)			Γ_{vib}	inv
J	K	Γ_{rot}	Γ_{tot}	E_{obs}	E_{calc}	obs–calc	CD
			(4 0 0 0 0 0 0)			A_1'	s
2	1	E″	E″	12681.2069	12680.5364	0.6705	−0.0030
3	0	A2′	A2′	12741.5406	12745.3641	−3.8235	0.0018
4	1	E″	E″	12812.1747	12814.5152	−2.3405	0.0002
4	3	A2″	A2″	12787.2347	12785.4952	1.7395	−0.0026
5	0	A2′	A2′	12916.2438	12918.2295	−1.9857	0.0060
5	3	A2″	A2″	12879.9778	12881.4929	−1.5151	0.0040
7	0	A2′	A2′	13162.1885	13163.9509	−1.7624	−0.0080
7	3	A2″	A2″	13121.4242	13124.2805	−2.8563	0.0024
			(4 1 0 0 0 0 0)			A_2''	a
1	1	E″	E′	12647.3807	12647.9248	−0.5441	0.0056
3	1	E″	E′	12739.5634	12742.1144	−2.5510	0.0030
4	1	E″	E′	12814.5824	12819.3480	−4.7656	0.0054
4	3	A1″	A2′	12792.7603	12792.6131	0.1472	−0.0042
5	3	A1″	A2′	12885.1122	12886.2266	−1.1144	0.0005
			(3 0 1 1 0 0 1)			E′	s
1	0	A2′	E′	12644.1652	12648.5232	−4.3580	0.0030
1	1	E″	A2″	12639.5608	12644.8754	−5.3146	−0.0005
2	0	A1′	E′	12687.1540	12687.8175	−0.6711	−0.0089
2	1	E″	A2″	12678.5295	12682.6027	−4.0732	0.0000
2	2	E′	E′	12668.3932	12671.7701	−3.3769	−0.0034
3	0	A2′	E′	12745.0456	12746.3841	−1.3385	0.0001
3	1	E″	E″	12735.2715	12740.3391	−5.0676	−0.0048
3	2	E′	A2′	12727.4345	12729.9911	−2.5566	−0.0077
3	3	A1″	E″	12708.3978	12711.1960	−2.7982	0.0037
3	3	A2″	E″	12714.9295	12712.8911	2.0384	
4	0	A1′	E′	12824.9357	12822.6577	2.2780	−0.0114
4	1	E″	A2″	12814.7190	12815.6976	−0.9786	−0.0001
4	2	E′	E′	12807.0338	12807.2047	−0.1709	0.0005
4	3	A2″	E″	12785.3973	12789.5558	−4.1585	−0.0096
4	3	A1″	E″	12787.3464	12790.2839	−2.9375	−0.0070
4	4	E′	A2′	12763.0284	12764.6944	−1.6660	0.0147
5	0	A2′	E′	12923.2247	12920.2978	2.9269	0.0005
5	1	E″	A2″	12918.9208	12919.1662	−0.2454	−0.0019
5	3	A1″	E″	12885.2745	12885.9037	−0.6292	−0.0042
5	4	E′	A2′	12859.0701	12861.1086	−2.0385	−0.0078
5	5	E″	E″	12825.3651	12827.0873	−1.7222	0.0053
6	1	E″	A2″	13024.0901	13021.9610	2.1291	−0.0120
6	4	E′	A2′	12969.8970	12972.3181	−2.4211	0.0101
6	5	E″	E″	12942.2937	12942.7868	−0.4931	−0.0089
6	6	A2′	E′	12901.1655	12902.3130	−1.1475	0.0087
7	2	E′	A2′	13134.2814	13137.3830	−3.1016	−0.0107
7	4	E′	A2′	13106.0133	13105.4539	0.5594	0.0108
7	6	A2′	E′	13033.1831	13036.9726	−3.7895	0.0087
7	7	E″	A2″	12981.8239	12987.4457	−5.6218	−0.0424
			(3 1 1 1 0 0 1)			E″	a
2	0	A1′	E″	12690.9603	12693.4573	−2.4970	−0.0015
2	2	E′	A2″	12675.3915	12678.4242	−3.0327	−0.0005
3	0	A2′	E″	12750.1264	12752.0289	−1.9025	−0.0006
3	1	E″	A2′	12743.1572	12741.6482	1.5090	−0.0008
3	2	E′	A2″	12736.9306	12736.8809	0.0497	−0.0066
3	3	A1″	E′	12716.5745	12718.7199	−2.1454	0.0009
3	3	A1″	E″	12714.9295	12712.8911	2.0384	
4	0	A1′	E″	12828.5337	12831.3404	−2.8067	−0.0114
4	3	A1″	E′	12794.2035	12796.4136	−2.2101	−0.0014
4	4	E′	A2″	12770.4277	12770.1520	0.2757	−0.0092
5	4	E′	A2″	12865.1930	12867.2502	−2.0572	0.0017
6	6	A1′	E″	12910.2129	12913.3883	−3.1754	0.0090
7	5	E″	E′	13081.4018	13080.2455	1.1563	0.0073
7	6	A2′	E″	13039.6539	13041.0064	−1.3525	−0.0073
			(2 0 2 0 0 0 0)			A_1'	s
3	3	A2″	A2′	12758.2776	12757.0767	1.2009	0.0083
5	3	A2″	A2′	12879.5548	12882.9411	−3.3863	0.0106
6	3	A2″	A2′	12998.7767	12995.2238	3.5529	−0.0105
			(2 1 2 0 0 0 0)			A_2''	a
3	3	A1″	A2′	12714.8479	12716.2008	−1.3529	−0.0091
4	0	A1′	A2″	12827.5305	12829.6757	2.1452	−0.0014
			(2 0 2 2 0 0 2)			E′	s
1	1	E″	E″	12647.3176	12644.9837	2.3339	
2	1	E″	E″	12681.5627	12684.8262	-3.2635	-0.0065
2	2	E′	A2′	12671.3482	12673.0216	-1.6734	
3	1	E″	A2″	12743.5516	12744.7400	-1.1884	-0.0014

(*continued on next page*)

Table 3 (*continued*)

3	2	E′	E′	12734.5993	12730.8776	3.7239	–0.0019
3	3	A2″	E″	12757.6429	12758.0402	-0.3973	-0.0063
4	1	E″	E″	12824.5018	12820.9249	3.5769	-0.0084
4	2	E′	A2′	12808.7399	12808.9749	-0.2350	-0.0002
5	2	E′	A2′	12897.9974	12899.8843	-1.8869	-0.0011
5	3	A2″	E″	12885.2737	12888.3453	-3.0716	-0.0044
5	4	E′	E′	12857.8481	12861.7550	-3.9069	0.0060
5	5	E″	A2″	12825.6466	12828.9782	-3.3316	0.0074
6	4	E′	E′	12975.9378	12976.1006	-0.1628	0.0010
6	6	A2′	E′	12941.7937	12940.5317	1.2620	-0.0002
7	7	E″	A2″	13022.6494	13026.3872	-3.7378	-0.0036
			(2 1 2 2 0 0 2)			E″	a
1	1	E″	A2′	12650.1021	12650.9560	-0.8539	-0.0026
2	0	A1′	E″	12695.4938	12694.6709	2.0365	-0.0047
2	1	E″	E′	12687.8105	12689.7044	1.6588	0.0113
2	2	E′	E″	12682.9105	12678.7430	4.1675	-0.0070
3	1	E″	A2′	12744.1854	12746.5713	-2.3859	0.0131
3	2	E′	A2″	12735.7747	12738.1795	-2.4048	0.0046
3	3	A2′	E′	12764.7351	12768.9027	-4.1677	-0.0002
4	2	E′	A2″	12809.9641	12811.3267	-1.3626	0.0030
4	4	E′	E″	12771.9820	12771.6080	0.3740	0.0078
5	3	A1″	E′	12890.6489	12891.0609	-0.4120	-0.0091
5	5	E″	E′	12835.8205	12834.8273	0.9932	0.0119
6	2	E′	A2″	13016.9328	13016.5572	0.3756	-0.0034
6	6	A2′	E″	12953.7506	12952.3551	1.3955	0.0069
7	7	E″	A2′	12993.2624	12995.3526	-2.0902	0.0119
			(1 0 3 1 0 0 1)			E′	s
2	1	E″	A2″	12734.2126	12737.6518	-3.4392	0.0076
2	2	E′	E′	12719.3683	12720.7418	-1.3735	0.0108
3	1	E″	E″	12742.5677	12745.0609	-2.4932	0.0054
4	0	A1′	E′	12824.2547	12827.0713	-2.8166	-0.0044
4	1	E″	A2″	12882.7271	12884.3506	-1.6235	0.0087
4	3	A1″	E″	12854.9341	12856.2817	-1.3476	-0.0009
4	4	E′	A2′	12806.3400	12806.7780	-0.4380	0.0047
5	4	E′	A2′	12910.6805	12913.6014	-2.9209	-0.0097
5	5	E″	E″	12865.5993	12868.2540	-2.6547	-0.0107
6	4	E′	A2′	12980.7688	12982.1619	-1.3931	0.0080
6	5	E″	A2″	12946.2953	12944.6633	1.6320	0.0006
7	5	E″	E″	13073.8825	13075.3003	-1.4178	0.0021
			(1 1 3 1 0 0 1)			E″	a
2	1	E″	A2′	12691.7132	12691.7132	-3.0945	
			(1 0 3 3 0 0 3)			A_1'	s
6	6	A2′	A2′	12948.6537	12947.7858	0.8679	0.0011
			(0 0 4 2 0 0 2)			E′	s
2	1	E″	E″	12746.1781	12743.4163	2.7618	-0.0104
2	2	E′	A2′	12729.1539	12730.9886	-1.8347	0.0020
3	1	E″	A2″	12807.3727	12804.3376	3.0351	
4	4	E′	A2′	12805.4602	12807.4511	-1.9909	0.0006
			(0 1 4 2 0 0 2)			E″	a
2	1	E″	A2′	12746.8972	12746.7285	0.1687	
3	1	E″	E′	12747.3957	12749.1734	-1.7777	0.0096
4	4	E′	A2″	12814.1741	12817.6458	-3.4717	0.0167
5	2	E′	A2″	12910.2687	12912.3785	-2.1098	-0.0069
6	5	E″	A2′	12953.1030	12955.3025	-2.1995	0.0129
			(0 0 4 4 0 0 4)			E′	s
3	2	E′	A2′	12792.5847	12789.2593	3.3254	-0.0084
6	5	E″	E″	12946.4735	12947.0277	-0.5542	0.0080
			(0 1 4 4 0 0 4)			E″	a
1	1	E″	A2′	12704.1513	12706.8491	-2.6978	-0.0095
2	2	E′	E″	12733.4999	12732.4950	1.0049	0.0093
3	2	E′	A2″	12804.9187	12802.8907	2.0280	-0.0009
5	4	E′	A2″	12925.7941	12923.4206	2.3735	0.0011
5	5	E″	E′	12875.8187	12878.6184	-2.7997	-0.0033

Analysis of the measured line positions was performed using combination differences (CDs), which gave 109 experimental energy levels. In addition to the lines assigned by CDs, the 10 strongest transitions in the calculated line list were assigned by choosing the strongest experimental lines and the average obs.-calc. value for the vibrational state in question. In all, 119 new experimental levels were determined from 278 measured line positions assigned to 300 transitions. The levels belong to 16 vibrational states arising from the third NH stretching overtone (ν_{NH}=4). The average precision of the CDs obtained equals 0.007 cm^{-1}, making the possibility of accidental agreement in difference between energy levels and frequencies about 3%.

Of the 928 lines measured in Prague there are 369 lines not observed in Brussels. We are able to assign 40 of these lines; in nearly all cases these are low intensity transitions with $I < 10^{-24}$. As these assignments must be regarded as less secure than the

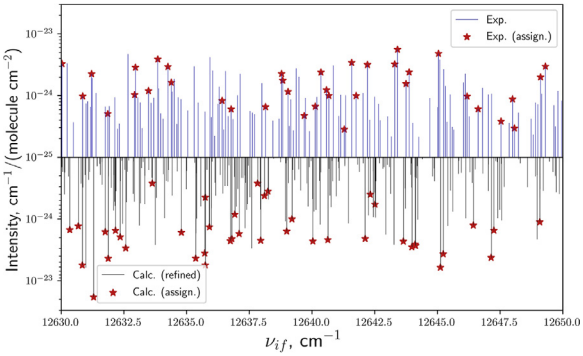

Fig. 5. Comparison of a portion of the calculated and observed room temperature spectra of ammonia with lines for which we provide assignments marked. The calculated lines are taken from a refined version of the line list of Coles et al. [52] which used empirical energy levels where available.

others, they have been marked with an asterisk in the file listing our assigned transitions is given in the supplementary material. This file contains quantum numbers of the assigned transitions together with their symmetries and line intensities, both observed and calculated. Table 3 gives energy levels derived from these experimental line positions. Fig. 5 gives a comparison of a portion of the observed and calculated spectra showing those lines for which assignments are obtained.

4. Conclusion

The absorption spectrum of ammonia near 0.793 μm has been recorded at high resolution using two Fourier transform spectrometers, in Brussels and Prague. The positions and intensities of a total of 1481 ammonia lines observed in the range 12491 – 12810 cm^{-1} have been measured. They were analyzed using an empirical line list computed using variational nuclear motion calculations and ground state combination differences. 278 of the observed lines were assigned to 300 transitions to vibrational states involving $4\nu_{NH}$ stretching excitation ($\nu_1 + \nu_3 = 4$) and 119 upper state energy levels were derived from these assigned line positions.

As a result of the present study, the main rotation-vibration bands of ammonia from the microwave to the green are now characterized experimentally. Extending this further, to the blue, the near ultraviolet and possibly up to dissociation, represents the next challenge both for experiment and theory. The spectroscopically-determined PES [52] used in this work was optimized by fitting to empirical energy levels up to 10 000 cm^{-1}. As Table 3 shows, the discrepancy between the levels calculated from this PES and the experimental values of this paper is a few wavenumbers. The inclusion of the experimental energy levels determined in this paper (see Table 3) to fit an new PES should significantly improve the extrapolation power of the PES and improve the accuracy of predictions of the optical NH_3 spectra as well as the spectra of ammonia towards dissociation. As our experience with water spectra up to dissociation shows [58], accurate knowledge of predicted, highly excited energy levels is vital for observation of levels at dissociation. In its turn, observation of the levels above 20 000 cm^{-1} will allow the construction of the first accurate, global PES of ammonia which is important for the production of an accurate NH_3 line list in near IR and optical region at high temperatures; such a line list is needed for the study of the atmospheres of planets and exoplanets.

Declaration of Competing Interest

None of the authors declare a conflict of interest.

Acknowledgement

This work was supported by the ERC Advanced Investigator Project 883830, the UK Natural Environment Research Council grant NE/T000767/1 and the Russian Fund for Fundamental Studies. RIO, VYuM, NFZ and OLP acknowledge support by State Project IAP RAS No. 0035-2019-0016. The work carried out in Prague is part of a research series funded by grant no. 19-03314S of the Czech Science Foundation and ERDF/ESF “Centre of Advanced Applied Sciences” (No. CZ.02.1.01/0.0/0.0/16_019/0000778). T. Bertin thanks the “Fonds pour la formation à la Recherche dans l’Industrie et dans l’Agriculture” (FRIA, Belgium) for a PhD fellowship. The authors are grateful to the two reviewers for their significant work in finding errors in our original assigments and improving the paper.

Supplementary material

Supplementary material associated with this article can be found, in the online version, at doi:10.1016/j.jqsrt.2021.107838.

References

[1] Cleeton CE, Williams NH. Electromagnetic waves of 1.1 cm wave-length and the absorption spectrum of ammonia. Physical Review 1934;45:234.
[2] Erisman JW, Galloway JN, Seitzinger S, Bleeker A, Dise NB, Petrescu AMR, Leach AM, de Vries W. Consequences of human modification of the global nitrogen cycle. Phil Trans R Soc B 2013;368:20130116. doi:10.1098/rstb.2013.0116.
[3] von Bobrutzki K, Braban CF, Famulari D, Jones SK, Blackall T, Smith TEL, et al. Field inter-comparison of eleven atmospheric ammonia measurement techniques. Atmos Meas Tech 2010;3:91–112. doi:10.5194/amt-3-91-2010.
[4] Galloway JN, Aber JD, Erisman JW, Seitzinger SP, Howarth RW, Cowling EB, Cosby BJ. The nitrogen cascade. Bioscience 2003;53:341–56. doi:10.1641/0006-3568(2003)053[0341:TNC]2.0.CO;2.
[5] Appl M. Ammonia, 2. production processes. American Cancer Society; 2011. doi:101002/14356007o02_o11.
[6] Schwieterman EW, Kiang NY, Parenteau MN, Harman CE, DasSarma S, Fisher TM, et al. Exoplanet biosignatures: a review of remotely detectable signs of life. Astrobiology 2018;18:663–708. doi:10.1089/ast.2017.1729.
[7] Lucas PW, Tinney CG, Burningham B, Leggett SK, Pinfield DJ, Smart R, Jones HRA, Marocco F, Barber RJ, Yurchenko SN, Tennyson J, Ishii M, Tamura M, Day-Jones AC, Adamson A, Allard F, Homeier D. The discovery of a very cool, very nearby brown dwarf in the galactic plane. Mon Not R Astron Soc 2010;408:L56–60.
[8] Leggett SK, Morley CV, Marley MS, Saumon D. Near-infrared photometry of y dwarfs: low ammonia abundance and the onset of water clouds. Astrophys J 2015;799:37. doi:10.1088/0004-637X/799/1/37.
[9] Irwin PGJ, Bowles N, Braude AS, Garland R, Calcutt S, Coles PA, Yurchenko SN, Tennyson J. Analysis of gaseous ammonia (NH_3) absorption in the visible spectrum of jupiter - update. Icarus 2019;321:572–82. doi:10.1016/j.icarus.2018.12.008.
[10] Beaulieu JP, Tinetti G, Kipping D, Ribas I, Barber RJ, Cho JY-K, et al. Methane in the atmosphere of the transiting hot Neptune GJ436b? Astrophys J 2011;731:16.
[11] Fortney J.J., Visscher C., Marley M.S., Hood C.E., Line M.R., Thorngren D.P., Freedman R.S., Lupu R.. Beyond equilibrium temperature: How the atmosphere/interior connection affects the onset of methane, ammonia, and clouds in warm transiting giant planets. 2020.
[12] Zobov NF, Shirin SV, Ovsyannikov RI, Polyansky OL, Yurchenko SN, Barber RJ, Tennyson J, Hargreaves R, Bernath P. Analysis of high temperature ammonia spectra from 780 to 2100 cm^{-1}. J Mol Spectrosc 2011;269:104–8. doi:10.1016/j.jms.2011.05.003.
[13] Hargreaves RJ, Li G, Bernath PF. Hot NH_3 spectra for astrophysical applications. Astrophys J 2012;735:111. doi:10.1088/0004-637X/735/2/111.
[14] Hargreaves RJ, Li G, Bernath PF. Ammonia line lists from 1650 to 4000 cm^{-1}. J Quant Spectrosc Radiat Transf 2012;113:670–9. doi:10.1016/j.jqsrt.2012.02.033.
[15] Barton EJ, Yurchenko SN, Tennyson J, Clausen S, Fateev A. High-resolution absorption measurements of NH_3 at high temperatures: 500 - 2100 cm^{-1}. J Quant Spectrosc Radiat Transf 2015;167:126–34. doi:10.1016/j.jqsrt.2015.07.020.
[16] Beale CA, Hargreaves RJ, Coles P, Tennyson J, Bernath PF. Infrared absorption spectra of hot ammonia. J Quant Spectrosc Radiat Transf 2017;203:410–16. doi:10.1016/j.jqsrt.2017.02.012.
[17] Rothman LS, Gordon IE, Barbe A, Benner DC, Bernath PF, Birk M, Boudon V, Brown LR, Campargue A, Champion JP, Chance K, Coudert LH, Dana V, Devi VM, Fally S, Flaud JM, Gamache RR, Goldman A, Jacquemart D, Kleiner I, Lacome N, Lafferty WJ, Mandin JY, Massie ST, Mikhailenko SN, Miller CE, Moazzen-Ahmadi N, Naumenko OV, Nikitin AV, Orphal J, Perevalov VI, Perrin A, Predoi-Cross A, Rinsland CP, Rotger M, Simeckova M, Smith MAH, Sung K, Tashkun SA, Tennyson J, Toth RA, Vandaele AC, Auwera JV. The *HI-*

TRAN 2008 molecular spectroscopic database. J Quant Spectrosc Radiat Transf 2009;110:533–72.
[18] Barton EJ, Yurchenko SN, Tennyson J, Béguier S, Campargue A. A near infrared line list for NH_3: analysis of a Kitt Peak spectrum after 35 years. J Mol Spectrosc 2016;325:7–12. doi:10.1016/j.jms.2016.05.001.
[19] Barton EJ, Polyansky OL, Yurchenko SN, Tennyson J, Civis S, Ferus M, Hargreaves R, Ovsyannikov I, Kyuberis AA, Zobov NF, Béguier S, Campargue A. Absorption spectra of ammonia near 1 μm. J Quant Spectrosc Radiat Transf 2017;203:392–7. doi:10.1016/j.jqsrt.2017.03.042.
[20] Zobov NF, Coles PA, Ovsyannikov RI, Kyuberis AA, Hargreaves RJ, Bernath PF, et al. Analysis of the red and green optical absorption spectrum of gas phase ammonia. J Quant Spectrosc Radiat Transf 2018;224–231:209. doi:10.1016/j.jqsrt.2018.02.001.
[21] Cacciani P, Čermák P, Béguier S, Campargue A. The absorption spectrum of ammonia between 5650 and 6350 cm^{-1}. J Quant Spectrosc Radiat Transf 2020. doi:10.1016/j.jqsrt.2020.107334.
[22] Wallace L, Bernath P, Livinston W, Hinkle K, Busler J, Guo BJ, et al. Water on the Sun. Science 1995;268:1155–8. doi:10.1126/science.7761830.
[23] Polyansky OL, Zobov NF, Viti S, Tennyson J, Bernath PF, Wallace L. Water in the Sun: line assignments based on variational calculations. Science 1997;277:346–9.
[24] Polyansky OL, Zobov NF, Viti S, Tennyson J, Bernath PF, Wallace L. K band spectrum of water in sunspots. Astrophys J 1997;489:L205–8.
[25] Polyansky OL, Zobov NF, Viti S, Tennyson J, Bernath PF, Wallace L. High temperature rotational transitions of water in sunspot and laboratory spectra. J Mol Spectrosc 1997;186:422–47.
[26] Drouin BJ, Yu S, Pearson JC, Gupta H. Terahertz spectroscopy for space applications: 2.5–2.7 THz spectra of HD, H_2O and NH_3. J Mol Struct 2011;1006:2–12.
[27] Yu S, Pearson JC, Drouin BJ, Sung K, Pirali O, Vervloet M, Martin-Drumel M-A, Endres CP, Shiraishi T, Kobayashi K, Matsushima F. Submillimeter-wave and far-infrared spectroscopy of high-j transitions of the ground and $\nu_2 = 1$ states of ammonia. J Chem Phys 2010;133:174317.
[28] Guinet M, Jeseck P, Mondelain D, Pepin I, Janssen C, Camy-Peyret C, Mandin JY. Absolute measurements of intensities, positions and self-broadening coefficients of R branch transitions in the ν_2 band of ammonia. J Quant Spectrosc Radiat Transf 2011;112:1950–60.
[29] Cermák P, Hovorka J, Veis P, Cacciani P, Cosléou J, Romh JE, Khelkhal M. Spectroscopy of $^{14}NH_3$ and $^{15}NH_3$ in the 2.3 μm spectral range with a new VECSEL laser source. J Quant Spectrosc Radiat Transf 2014;137:13–22.
[30] Földes T, Golebiowski D, Herman M, Softley TP, Di Lonardo G, Fusina L. Low-temperature high-resolution absorption spectrum of $^{14}NH_3$ in the $\nu_1 + \nu_3$ band region (1.51 μm). Mol Phys 2014;112:2407–18.
[31] Vander Auwera J, Vanfleteren T. Line positions and intensities in the 7400–8600 cm^{-1} region of the ammonia spectrum. Mol Phys 2018;116:3621–30. doi:10.1080/00268976.2018.1467054.
[32] Sung K, Brown LR, Huang X, Schwenke DW, Lee TJ, Coy SL, Lehmann KK. Extended line positions, intensities, empirical lower state energies and quantum assignments of $^{14}NH_3$ from 6300 to 7000 cm^{-1}. J Quant Spectrosc Radiat Transf 2012;113:1066–83. doi:10.1016/j.jqsrt.2012.02.037.
[33] Gordon IE, Rothman LS, Hill C, Kochanov RV, Tan Y, Bernath PF, Birk M, Boudon V, Campargue A, Chance KV, Drouin BJ, Flaud J-M, Gamache RR, Hodges JT, Jacquemart D, Perevalov VI, Perrin A, Shine KP, Smith M-AH, Tennyson J, Toon GC, Tran H, Tyuterev VG, Barbe A, Császár AG, Devi VM, Furtenbacher T, Harrison JJ, Hartmann J-M, Jolly A, Johnson TJ, Karman T, Kleiner I, Kyuberis AA, Loos J, Lyulin OM, Massie ST, Mikhailenko SN, Moazzen-Ahmadi N, Müller HSP, Naumenko OV, Nikitin AV, Polyansky OL, Rey M, Rotger M, Sharpe SW, Sung K, Starikova E, Tashkun SA, Auwera JV, Wagner G, Wilzewski J, Wcisło P, Yu S, Zak EJ. The *HITRAN* 2016 molecular spectroscopic database. J Quant Spectrosc Radiat Transf 2017;203:3–69. doi:10.1016/j.jqsrt.2017.06.038.
[34] Coles PA, Yurchenko SN, Kovacich RP, Hobby J, Tennyson J. A variationally computed room temperature line list for AsH_3. Phys Chem Chem Phys 2019;21:3264–77. doi:10.1039/C8CP07110A.
[35] Derzi ARA, Furtenbacher T, Yurchenko SN, Tennyson J, Császár AG. MARVEL Analysis of the measured high-resolution spectra of $^{14}NH_3$. J Quant Spectrosc Radiat Transf 2015;161:117–30. doi:10.1016/j.jqsrt.2015.03.034.
[36] Furtenbacher T, Coles PA, Tennyson J, Yurchenko SN, Yu S, Drouin B, Tóbiás R, Császár AG. Empirical rovibational energy of ammonia up to 7500 cm^{-1}. J Quant Spectrosc Radiat Transf 2020;251:107027. doi:10.1016/j.jqsrt.2020.107027.
[37] Coy SL, Lehmann KK. Rotational structure of ammonia N-H stretch overtones: five and six quanta bands. J Chem Phys 1986;84:5239–49.
[38] Lehmann KK, Coy SL. Spectroscopy and intramolecular dynamics of highly excited vibrational states of NH_3. J Chem Soc Faraday Trans II 1988;84:1389–406.
[39] Coy SL, Lehmann KK. Modeling the rotational and vibrational structure of the i.r. optical spectrum of NH_3. Spectrochim Acta 1989;45A:47–56.
[40] Kuga T, Shimizu T, Ueda Y. Observation and analysis of visible overtone band transitions of NH_3. Jap J Appl Phys 1985;24:L147.
[41] Giver LP, Miller JH, Boese RW. A laboratory atlas of the $5\nu_1$ NH_3 absorption band at 6475 Å with applications to Jupiter and Saturn. Icarus 1975;25:34–48. doi:10.1016/0019-1035(75)90187-6.
[42] Carleer M. WSPectra: a windows program to accurately measure the line intensities of high-resolution fourier transform spectra. In: Russel JE, Schäfer K, Lado-Bordowsky O, editors. Remote Sensing of Clouds and the Atmosphere V, Vol. 4168 of Proceedings of SPIE – The International Society for Optical Engineering; 2001. p. 337.
[43] Tudorie M, Foldes T, Vandaele A, Vander Auwera J. CO_2Pressure broadening and shift coefficients for the 1–0 band of HCl and DCl. J Quant Spectrosc Radiat Transf 2012;113:1092–101.
[44] Daneshvar L, Foldes T, Buldyreva J, Vander Auwera J. Infrared absorption by pure CO_2 near 3340 cm^{-1}: measurements and analysis of collisional coefficients and line-mixing effects at subatmospheric pressures. J Quant Spectrosc Radiat Transf 2014;149:258–74.
[45] Bernardo C, Griffith D. Fourier transform spectrometer instrument lineshape (ILS) retrieval by fourier deconvolution. J Quant Spectrosc Radiat Transf 2005;95:141–50.
[46] Wells R. Rapid approximation to the Voigt/Faddeeva function and its derivatives. J Quant Spectrosc Radiat Transf 1999;62:29–48.
[47] Markov VN, Pine AS, Buffa G, Tarrini O. Self broadening in the ν_1 band of NH_3. J Quant Spectrosc Radiat Transf 1993;50:167–78.
[48] Aroui H, Nouri S, Bouanich JP. NH_3Self-broadening coefficients in the $\nu 2$ and $\nu 4$ bands and line intensities in the $\nu 2$ band. J Mol Spectrosc 2003;220:248–58.
[49] Aroui H, Laribi H, Orphal J, Chelin P. Self-broadening, self-shift and self-mixing in the $\nu 2$, $2\nu 2$ and $\nu 4$ bands of NH3. J Quant Spectrosc Radiat Transf 2009;110:2037–59.
[50] Sung K, Brown L, Huang X, Schwenke D, Lee T, Coy S, Lehmann K. Extended line positions, intensities, empirical lower state energies and quantum assignments of NH_3 from 6300 to 7000 cm^{-1}. J Quant Spectrosc Radiat Transf 2012;113:1066–83.
[51] Maaroufi N, Jalleli C, Tchana FK, Landsheere X, Aroui H. Absolute line intensities and first measurements of self-collisional broadening and shift coefficients in the $2\nu_4$ band of NH_3. J Quant Spectrosc Radiat Transf 2018;354:24–31.
[52] Coles PA, Ovsyannikov RI, Polyansky OL, Yurchenko SN, Tennyson J. Improved potential energy surface and spectral assignments for ammonia in the near-infrared region. J Quant Spectrosc Radiat Transf 2018;219:199–212. doi:10.1016/j.jqsrt.2018.07.022.
[53] Polyansky OL, Ovsyannikov RI, Kyuberis AA, Lodi L, Tennyson J, Yachmenev A, Yurchenko SN, Zobov NF. Calculation of rotation-vibration energy levels of the ammonia molecule based on an *ab initio* potential energy surface. J Mol Spectrosc 2016;327:21–30. doi:10.1016/j.jms.2016.08.003.
[54] Yurchenko SN, Thiel W, Jensen P. Theoretical ROVibrational energies (TROVE): arobust numerical approach to the calculation of rovibrational energies for polyatomic molecules. J Mol Spectrosc 2007;245:126–40. doi:10.1016/j.jms.2007.07.009.
[55] Yurchenko SN, Barber RJ, Yachmenev A, Thiel W, Jensen P, Tennyson J. A variationally computed t=300 k line list for NH_3. J Phys Chem A 2009;113:11845–55. doi:10.1021/jp9029425.
[56] Down MJ, Hill C, Yurchenko SN, Tennyson J, Brown LR, Kleiner I. Re-analysis of ammonia spectra: updating the HITRAN $^{14}NH_3$ database. J Quant Spectrosc Radiat Transf 2013;130:260–72. doi:10.1016/j.jqsrt.2013.05.027.
[57] Urban Š, Papoušek D, Devi VM, Fridovich B, D'Cunha R, Rao KN. Transition dipole matrix elements for $^{14}NH_3$ from the line intensities of the $2\nu_2$ and ν_4 bands. J Mol Spectrosc 1984;106:38–55.
[58] Grechko M, Boyarkin OV, Rizzo TR, Maksyutenko P, Zobov NF, Shirin S, Lodi L, Tennyson J, Császár AG, Polyansky OL. State-selective spectroscopy of water up to its first dissociation limit. J Chem Phys 2009;131:221105.